Characterization of the Cellular Respiration & Mitochondrial Metabolism in C2C12 Mouse Myoblasts

by
Bergen Sather

A THESIS

submitted to

Oregon State University

Honors College

in partial fulfillment of
the requirements for the
degree of

Honors Baccalaureate of Science in Biology
(Honors Scholar)

Presented May 18, 2018
Commencement June 2018

AN ABSTRACT OF THE THESIS OF

Bergen Sather for the degree of Honors Baccalaureate of Science in Biology presented on May 18, 2018. Title: Characterization of the Cellular Respiration & Mitochondrial Metabolism in C2C12 Mouse Myoblasts.

Abstract approved:_____

Sean Newsom

Type-2 diabetes (T2D) has become a pandemic. The main impairment in T2D is skeletal muscle insulin resistance (IR) and is often associated with obesity. Despite decades of study, the mechanisms of IR have not been fully resolved. Evidence has implicated mitochondrial dysfunction as a potential cause and/or consequence of IR. A potential contributing factor is a lower ability for mitochondria to oxidize lipid substrates, particularly in the presence of other competing substrates. C2C12 mouse myoblasts are a common model used to study IR and T2D in muscle, but their intrinsic respiration patterns are unknown. We investigated the cellular respiration and mitochondrial metabolism of the C2C12 myoblast cell line in the presence of lipid and non-lipid substrates. With the use of high-resolution respirometry, we learned C2C12 myoblasts exhibit a reduced capacity to oxidize lipids compared to other substrates, but no major mitochondrial defects. These data indicate the capacity for mitochondria to oxidize lipids is lower than the total respiratory capacity of C2C12 cells, suggesting that limitations in skeletal lipid oxidation may be upstream of the electron transport system. Such characterization of C2C12 myoblasts can help identify potential regulatory factors for mitochondrial fuel metabolism in future studies using this cell line in the study of IR, T2D and mitochondrial dysfunction.

Key Words: type-2 diabetes, insulin resistance, mitochondrial metabolism, C2C12 myoblasts

Corresponding e-mail address: satherb@oregonstate.edu

Characterization of the Cellular Respiration & Mitochondrial Metabolism of C2C12 Mouse Myoblasts

by
Bergen Sather

A THESIS

submitted to

Oregon State University

Honors College

in partial fulfillment of
the requirements for the
degree of

Honors Baccalaureate of Science in Biology
(Honors Scholar)

Presented May 18, 2018
Commencement June 2018

Honors Baccalaureate of Science in Biology project of Bergen Sather presented on May 18, 2018.

APPROVED:

_____

Sean Newsom, Mentor, representing Biological & Population Health Sciences

_____

Matt Robinson, Committee Member, representing Biological & Population Health Sciences

_____

Indira Rajagopal, Committee Member, representing Biochemistry & Biophysics

_____

Toni Doolen, Dean, Oregon State University Honors College

I understand that my project will become part of the permanent collection of Oregon State University, Honors College. My signature below authorizes release of my project to any reader upon request.

_____

Bergen Sather, Author

INTRODUCTION

Diabetes is considered a pandemic. In 2013, it was responsible for 5.1 million deaths; costing around 263 billion USD in American and Caribbean nations alone (Gonzalez 2017). Type 2 diabetes (T2D) accounts for about 90% of diabetes cases and is characterized by high concentrations of plasma glucose despite normal or increased insulin concentrations. Skeletal muscle is the largest insulin-responsive tissue in the body, with elevated blood glucose in T2D largely determined by an impaired ability of insulin to stimulate glucose uptake into skeletal muscle cells (Rizza 1981). Such decreased sensitivity to insulin is termed insulin resistance (IR) (Gonzalez 2017). Importantly, obesity increases risk for the development of IR, prediabetes and T2D. Despite many years of study, the mechanisms of IR in obesity are not fully resolved. Understanding the mechanisms regulating skeletal muscle insulin action with obesity may help the development of treatments designed to prevent, treat or reverse T2D.

Altered mitochondrial metabolism has been implicated in the development of obesity, IR, and progression to T2D. Mitochondria are critical regulators of cellular energy balance. They are the primary organelles for the production of energy from glucose and fatty acid oxidation (FAO). In skeletal muscle, the metabolism of both these substrates has been shown to be impaired in T2D (Kelley 2002). Energy balance is disrupted in obesity as a result of the level of available fuels exceeding that of energy demand. Obesity is closely linked with the development of IR and T2D, and declines in insulin sensitivity are associated with fat accumulation in tissues such as skeletal muscle (Covington 2017).

Obesity has been implicated in the development of metabolic dysregulation which includes decreased insulin sensitivity and impaired substrate switching (Koves 2008). There are numerous hypotheses linking increased fatty acid accumulation and mitochondrial dysfunction/IR. In obesity, there is an increased dependence on FAO (Di Meo 2017) that may lead to the accumulation of lipid metabolites or incompletely oxidized lipids as a result of high flux rates through oxidative pathways. It is possible that mitochondria are not capable of oxidizing all of the extra lipids and contribute to an accumulation of intramuscular lipids (Befroy 2007). Besides storage as triacylglycerols, muscle mitochondria do not often use other methods of handling fatty acids such as packaging, ketogenesis, lipogenesis, gluconeogenesis and glycerolipid synthesis compared to tissues such as the liver and may be susceptible to the presence of excess nutrient conditions associated with obesity (Koves 2008). The accumulation of lipid products may cause oxidative stress, mitochondrial damage, and reduced mitochondrial oxidative capacity (Gonzalez 2017). If mitochondria are impaired in their ability to convert fuels into energy, this may exacerbate accumulation of lipids. This is cause for concern because certain classes of lipids such as diacylglycerols and ceramides have been shown to interfere with the insulin signaling cascade, resulting in IR (Gonzalez 2017). Taken together, mitochondrial dysfunction in skeletal muscle is a major concern in the study of IR and T2D and further clarification of the possible link between IR and mitochondrial metabolism in skeletal muscle is needed.

Despite many studies demonstrating an association between IR and mitochondrial dysfunction, impaired mitochondrial function and insulin sensitivity are not consistently associated (Gonzalez 2017). Studies have shown no change (Lalia 2016),

or even increased oxidative phosphorylation (OxPHOS) activity despite IR (Lanza 2013). Others findings indicate mitochondrial metabolism may be increased during obesity (Hancock 2008; Newsom 2017). We recently reported no signs of mitochondrial defects measured with high resolution respirometry of animals on a high fat diet compared to low fat, despite IR (Newsom 2017). Others have questioned the timeline of the development of mitochondrial dysfunction and IR, asking whether mitochondrial dysfunction is a cause or consequence of IR (Gonzalez 2017). Evidence that mitochondria are not dysfunctional or that mitochondrial dysfunction may not play a direct role in the development of IR contributes to the need for continued investigation in this area. To better understand these relationships, we contend that we must first improve our understanding of mitochondrial function in working models of skeletal muscle metabolism. Studying the regulation of mitochondrial metabolism is necessary to gain this better understanding and can be done by evaluating mitochondrial metabolism in skeletal muscle cells that are often used to study IR.

Characterizing cellular respiration and mitochondrial metabolism in skeletal muscle cells is important for understanding the etiology of IR and T2D. Rodent and cell culture models are helpful for understanding mechanisms of metabolic control due to similarities of disease progression and signaling pathways with human physiology, yet avoid confounding factors and variability that can occur with human studies (Gonzalez 2017). Therefore, it is helpful to use skeletal muscle model systems such as C2C12 mouse myoblasts to study the relationship between mitochondrial dysfunction and IR. However, the intrinsic mitochondrial respiration characteristics of these cells remain poorly understood. To accurately interpret the results of future studies related to mitochondrial metabolism and IR with C2C12 myoblasts, a better understanding of the respiration patterns and mitochondrial metabolism of these cells is needed. This will allow for detection of potential changes in respiration and function in IR and T2D states.

The purpose of this investigation was to characterize the cellular respiration and mitochondrial metabolism of C2C12 mouse myoblasts to identify the intrinsic respiration profile of cells that are commonly used as a model to investigate the mechanisms of IR in skeletal muscle. The use of model systems to study IR and T2D in muscle cells is necessary to investigate the mechanisms of IR and the relationship between IR and mitochondrial dysfunction. Understanding the intrinsic respiration and mitochondrial metabolism of these model systems will help determine potential limitations of respiration and changes in respiratory functions with IR and T2D.

Using high resolution respirometry, we examined the capacity for the C2C12 myoblasts to oxidize various substrates of cellular respiration. Respiration was measured in the presence of lipid and non-lipid substrates and then the combined effects used to determine the contribution of multiple substrates to respiration. Simultaneous measures of mitochondrial reactive oxygen species (ROS) production were also completed. Western blot techniques were used to measure the presence of complexes of the electron transfer system (ETS). These data will help us better understand the mitochondrial metabolism of a model used to investigate IR and T2D so that we can ensure appropriate interpretation of further experiments using C2C12 myoblasts.

METHODS

Cell culture

C2C12 mouse myoblasts obtained from American Type Culture Collection (ATCC) were cultured according to ATCC recommendations. All culture media and reagents were purchased from Gibco. Cells were cultured at a humidified 37 °C and 5% CO_2 in T75 flasks using growth media (Dulbecco's Modified Eagle's Medium [DMEM] including 4.5g/L glucose, 0.584 g/L L-glutamine, 110 mg/L sodium pyruvate, supplemented with 10% fetal bovine serum and 1% antibiotic-antimycotic). As needed, cells were passed upon reaching ~80-90% confluency. Cells were rinsed with Dulbecco's Phosphate Buffered Saline (DPBS) to eliminate any residual serum, then incubated in 0.25% trypsin-EDTA for 5 min to suspend the cells. Growth media was added to inactivate the trypsin and to recover the suspended cells. Cells were pelleted by light centrifugation (180 x *g* for 5 minutes) at room temperature. Supernatant was aspirated and the cell pellet was re-suspended in growth media to be distributed in new T75 flasks. Cells were passed at ratios of 1:4-8, with no more than 5 passages prior to being harvested for experiments.

Cell harvest for respirometry experiments

C2C12 mouse myoblasts were harvested for respirometry experiments similar to the passage procedure described above. Upon achieving ~80% confluency, four T75 flasks were rinsed with DPBS, suspended using trypsin, diluted in growth media and pelleted via centrifugation (exactly as described above). However, to remove growth media from the cells, each cell pellet was rinsed and re-suspended in DPBS before being re-pelleted via centrifugation (180 x *g* for 5 minutes). After spinning, DPBS was aspirated and all 4 cell pellets were combined by re-suspending in 1 mL of MiR05 respiration buffer (0.5 mM EGTA, 3 mM MgCl2-6H2O, 60 mM Lactobionic acid, 20 mM taurine, 10 mM KH2PO4, 20 mM HEPES, 110 mM sucrose, 1 g/L bovine serum albumin). Cells were counted using a hemacytometer in order to achieve a consistent concentration for all of the respirometry experiments. 10µL of the cell suspension was diluted 1:10 in PBS, with 10 µL of the diluted cell suspension added to the hemacytometer. The four corner squares were counted and averaged. Cells were diluted to 4 million cells per mL and 250 µL of this suspension was added to each chamber of the O2k (i.e., 1 million cells per chamber).

Cell harvest for western blot analysis

Cell suspensions used in respirometry experiments (detailed below) were collected at the conclusion of those experiments for subsequent mitochondrial protein analysis via western blot analysis. The benefit of this approach is that these samples are the same cells used in the respiratory experiments. However, the low protein abundance and lack of protease inhibitors in these suspensions may result in suboptimal western blot analysis. Additional cell culture experiments were carried out to collect cell lysates under ideal conditions. Cells were cultured as previously described above, but ultimately passaged to 6-well plates in order to produce several replicates. When cells were ~90% confluent they were harvested in lysis buffer (20mM Tris-HCL (pH 7.5), 150mM NaCl, 1mM Na2EDTA, 1mM EGTA, 1% Triton, 2.5 mM sodium pyrophosphate, 1mM β-glycerophosphate, 1 mM Na3VO4 and 1% Protease inhibitor cocktail). The 6-well plates were removed from the incubator and placed on ice, growth media was poured off and the wells were washed twice with ice-cold PBS. 80 µL of lysis buffer was added to each well and cell scrapers were used to remove cells from the plate. Lysates were left on ice for 10 minutes. Tubes were then centrifuged at 10,000 x *g* for 10 minutes at 4 °C. Supernatant was collected and frozen at -80 °C.

High-resolution respirometry

High-resolution respirometry was performed using the Oxygraph O2k system (Oroboros Instruments, Innsbruck, Austria) with MiR05 respiration buffer. By performing multiple protocols, the O2k can offer a detailed measurement of different respiration states and a characterization of the intrinsic respiration profile of the C2C12 myoblasts (Gnaiger 2014). The Oxygraph has sealed chambers fitted with polarographic oxygen sensors that determine oxygen consumption as a function of changes in oxygen concentration (Horan 2012). The chambers are equipped with injection ports for titration of substrates, uncouplers, or inhibitors to test different aspects of cellular respiration. Additionally, the O2k can simultaneously measure H_2O_2 production to determine the production of ROS during respiration using fluorometry to detect the oxidation of resorufin (Amplex® Red, ThermoFisher Scientific) in the presence of horseradish peroxidase and superoxide dismutase.

Three different protocols were performed to measure substrate specific OxPHOS and determine the contribution of each complex of the ETS. The ETS capacity is measured after addition of an uncoupler and determines excess electron transfer capacity that is not used to generate ATP (usually exceeding OxPHOS). Each protocol offers a measurement of OxPHOS and ETS capacity in the presence of different substrates or different combinations of substrates. The titration of glutamate-malate-succinate (GMS, Table 1) measures respiration of N-linked (glutamate+malate) and S-linked respiration (succinate); these are related to electron transfer at complexes I and II, respectively. Palmitoylcarnitine and malate (PCM, Table 2) measures F-linked respiration; this is related to FAO and shuttles electrons to the ETS through the electron-transferring flavoprotein complex (CETF) and complex I. A reference protocol (RP2, Table 3) measures of all of these substrates together in order to test saturation of OxPHOS and the ETS.

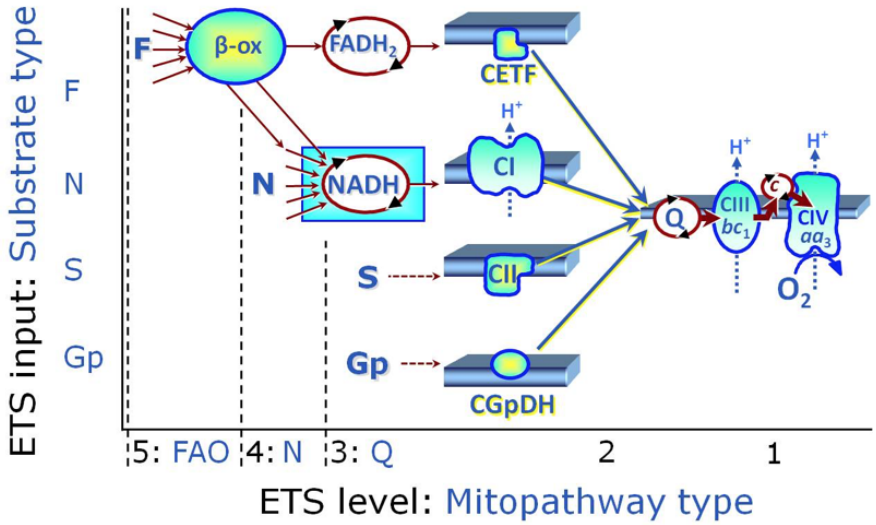

Figure 1. The pathways to the Q-junction image is adapted from the open access MiPNet Publications 2014 (Oroboros Instruments Corp). It outlines where the substrates of respiration are produced and how each one supplies reducing equivalents the Q-junction of the electron transfer system.

Table 1. Titration sequence, nomenclature, and brief description of respiratory states for GMS protocol. Concentrations are indicated for the total 2 ml volume of the respiratory chamber. (Newsom 2017)

Event	Respiration State	Description/Pathway

H_2O_2 production reagents: 10 µM amplex red, 5 U/ml superoxide dismutase, 1 U/ml horseradish peroxidase, and calibrated using injections of H_2O_2	n/a	For H_2O_2 production measurement. This determines reactive oxygen species (ROS) production after the addition of each substrate, which can indicate potential sources of mitochondrial damage
Cells 1 million cells per chamber (250 µL)	n/a	Digitonin was added to the cells at a concentration of 1.5 µL per million cells before injection into the O2k in order to permeabilize the plasma membranes
Oxidative Phosphorylation (OxPHOS)		
GM+ADP 10 mM glutamate 2 mM malate 5 mM ADP	P(N)	Glutamate and malate are N-linked substrates (NADH) that feed into the Q-junction through Complex I. Saturated concentration of ADP allows for OxPHOS (not limited by ADP) of N-linked respiration (Complex I)
Succ 10 mM succinate	P(N+S)	N-linked and S-linked respiration (Complex I + Complex II)
Cyto 10 µM cytochrome c	P(N+S)c	Cytochrome c test determines membrane integrity (oxygen consumption should not exceed that of the previous state) Cytochrome c is not compatible with amplex red and therefore H_2O_2 measurements were stopped after the addition of cytochrome c
Leak		
Oligo 2 µg/ml oligomycin	L(N+S)	Leak oxygen flux in the absence of functional ATP synthase (inhibited by oligomycin). This is a non-phosphorylating state, compensating for proton leak. Considered dissipative respiration (related to heat production)
Electron Transfer System (ETS)		
FCCP sequential additions of 0.05 mM FCCP to plateau	E(N+S)	Membrane integrity disrupted by FCCP, ETS capacity in the presence of N-linked and S-linked substrates
Rot 0.5 µM rotenone	E(S)	Electron transfer capacity of Complex II in the presence of N-linked and S-linked substrates with rotenone inhibiting Complex I

AA 2.5 mM antimycin A	ROX	Residual oxygen consumption with the inhibition of the ETS by antimycin A

Table 2. Titration sequence, nomenclature, and brief description of respiratory states for PCM protocol. Concentrations are indicated for the total 2 ml volume of the respiratory chamber**.** (Newsom 2017)

Event	**Respiration State**	**Description**
H_2O_2 production reagents 10 µM amplex red, 5 U/ml superoxide dismutase, and 1 U/ml horseradish peroxidase and calibrated using injections of H_2O_2	n/a	For H_2O_2 production measurement. This determines reactive oxygen species (ROS) production after the addition of each substrate, which can indicate potential sources of mitochondrial damage
Cells 1 million cells per chamber (250 µL)	n/a	Digitonin was added to the cells at a concentration of 1.5 µL per million cells before injection into the O2k in order to permeabilize the plasma membranes
PalmMal 0.005 mM palmitoyl-L-carnitine 2 mM malate	L(F)	Palmitate is an F-linked substrate that feeds electrons through both CETF and Complex I to the Q-junction
Oxidative Phosphorylation (OxPHOS)		
ADP 5 mM ADP	P(F)	Saturated concentration of ADP allows for oxidative phosphorylation of F-linked respiration (CETF + Complex I) from FAO of palmitate
Cyto 10 µM cytochrome c	P(F)c	Cytochrome c test determines membrane integrity (oxygen consumption should not exceed that of the previous state). Cytochrome c is not compatible with amplex red and therefore H_2O_2 measurements were stopped after the addition of cytochrome c.
Leak		
Oligo 2 µg/ml	L(F)	Leak oxygen flux in the absence of functional ATP synthase (inhibited by oligomycin). Non-phosphorylating state, compensation for proton leak, dissipative respiration (related to heat production)

Electron Transfer System (ETS)		
FCCP sequential additions of 0.05 mM FCCP to plateau	E(F)	Electron transfer system capacity in the presence of F-linked and N-linked substrates
AA 2.5 mM antimycin A	ROX	Residual oxygen consumption with the inhibition of the ETS by antimycin A

Table 3. Titration sequence, nomenclature, and brief description of respiratory states for Reference Protocol 2 (RP2). Concentrations are indicated for the total 2 ml volume of the respiratory chamber. (Oroboros 2018)

Event	Respiration State	Description
R	R	Routine respiration, limited to endogenous substrate supply and ATP demand, before plasma membranes have been permeablized with digitonin
ADP 5 mM ADP 4.1 µM digitonin	n/a	After addition of digitonin which is a detergent that permeablizes the cell plasma membranes to allow substrates to reach the mitochondria and ADP to allow for OxPHOS
Low Mal 0.1 mM malate (low)	n/a	Low concentration of malate titrated to support FAO. (malate can drive respiration on its own and thus a high concentration can inhibit the measurement of other substrates)
Oxidative Phosphorylation (OxPHOS)		
Oct 0.5 mM octanoyl carnitine	F(P)	Octanoyl carnitine is an F-linked substrate that enters the Q-junction through both CETF and Complex I through fatty acid oxidation (FAO)
Cyto 10 uM cytochrome c	F(P)c	Cytochrome c test to determine membrane integrity (oxygen consumption should not exceed that of the previous state)
Mal 2 mM malate (high)	F+N(P)	A higher concentration of malate is added to ensure that it is not limiting respiration (malate is N-linked and enters the Q-junction through Complex I)
Pyr 5 mM pyruvate	F+N(P)	Pyruvate is another N-linked substrate that enters the Q-junction through Complex I
Glut 10 mM glutamate	F+N(P)	Glutamate is another N-linked substrate that enters the Q-junction through Complex I

Succ 50 mM succinate	F+N+S(P)	Succinate is a S-linked substrate that enters the Q-junction through Complex II, oxygen consumption is now including electron flow through Complex I + Complex II + CETF
Gp 10 mM glycerol 3-phosphate	F+N+S+Gp(P)	Glycerol phosphate is a Gp-linked substrate that enters the Q-junction through CGpDH (Complex I + Complex II + CETF + CGpDH)
Electron Transfer System (ETS)		
FCCP sequential additions of 0.05 mM FCCP to plateau	F+N+S+Gp(E)	Uncoupled respiration using FCCP (disrupts membrane integrity) measures ETS capacity with all substrates present
Rot 0.5 uM rotenone	S+Gp(E)	Electron transfer capacity in the presence of all substrates (Complex I inhibited by rotenone, electron flow only through CETF + Complex II + CGpDH)
AA 2.5 uM antimycin A	ROX	Residual oxygen consumption with the inhibition of the ETS by antimycin A

Figure 2. Representative Oxygraph tracing of RP2 with oxygen concentration (blue line, left axis) and oxygen consumption (red line, right axis) over time. Titrations are indicated with vertical lines and respective nomenclature.

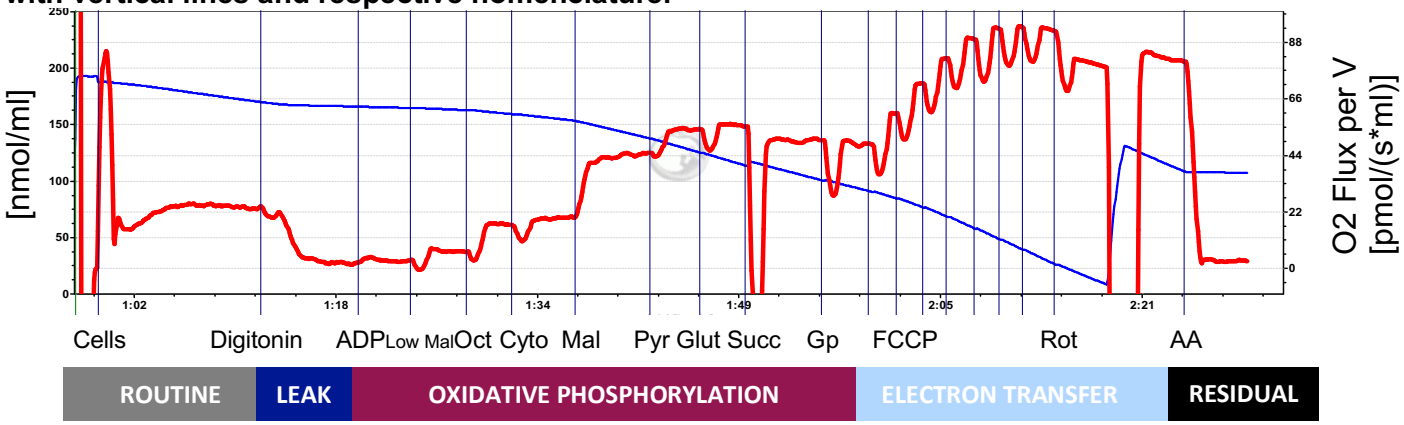

Western blot

Bicinchonic acid (BCA) assays were completed on recovered respirometry cell suspensions and cell lysates to determine protein concentrations of each sample. Sample was diluted in MiR05 respiration buffer (for samples recovered from respiration experiments) or lysis buffer (for cell lysates) to normalize protein concentrations. Laemmli sample buffer (BioRad) with 10% 2-mercaptoethanol (Fisher) was added to denature proteins. Samples were only warmed to 37 °C to preserve mitochondrial complex epitope recognition. Approximately 60 µg of protein from the cell lysates (or 22.5 µg from the samples retrieved from the Oxygraphs) were separated on 12% Bis-Tris gels then transferred to nitrocellulose membranes. Equal loading was verified using ponceau staining of membranes and tubulin as loading control. Membranes were blocked in 5%

bovine serum albumin in tris-buffered saline with tween (TBST) then incubated overnight at 4°C in primary antibodies (1:1000). Membranes were washed 3 × 10 minutes in TBST then incubated for 1 hour at room temperature in secondary antibody diluted in blocking buffer. Membranes were washed 3 × 5 minutes in TBST, followed by 3 × 5 minutes in TBS. Proteins of interest were visualized using infrared imaging (Odyssey, Licor, Lincoln NE). Primary antibodies were Tubulin (Licor #926-42213) used as a loading control, and Oxphos Cocktail (Abcam #110413) used to measure complexes of the electron transfer system that were tested in the respiratory experiments. Secondary antibodies were anti-rabbit-700 (1:10,000, Licor #926-68071) and anti-mouse-800 (1:10,000, Licor #926-32212).

Statistical analysis

Statistics were performed using JMP Pro v. 12.0 (SAS Institute Inc., Cary, NC). Graphs were generated using Prism v.6 (GraphPad Software Inc., La Jolla, CA). One-way analysis of variance (ANOVA) was used to compare respiratory experiments and pair-wise comparisons for were made using Tukey adjustment. Statistical significance was set at $P < 0.05$.

RESULTS

Mitochondrial Respiration

GMS: To test mitochondrial respiration, C2C12 myoblasts were provided with saturating levels of N-linked substrates (glutamate and malate) and S-linked substrate (succinate). Maximal OxPHOS was stimulated with a saturating level of ADP. OxPHOS capacity of N+S-Linked substrates exceeded that of N-Linked alone (Figure 3A,C). The cytochrome c test exhibited no change in respiration (<10% increase, P=0.6 for ADP vs. Cyto), demonstrating that mitochondrial membranes were intact (Figure 3A). Inhibition of ATP synthase with oligomycin decreased respiration to a leak state in which oxygen consumption decreased to 11±2% of maximal OxPHOS (Figure 3B), revealing that there is a small component of oxygen consumption that can be attributed to dissipation of the proton gradient created by the ETS. This represents oxygen consumption that is not being used to generate ATP. To test ETS capacity, the mitochondria were uncoupled with FCCP. FCCP dissipates the mitochondrial membrane potential by allowing enhanced translocation of protons across the membrane, increasing respiration as a result of increased electron flow to maintain membrane potential. In this state, oxygen consumption exceeded maximal OxPHOS by 31±4% (Figure 3A,B). This state is maximal oxygen consumption that is not limited by phosphorylation. Treatment with rotenone, a complex I inhibitor, decreased ETS capacity 49±6% (Figure 3D), demonstrating that complexes I and II were each contributing to approximately half of the ETS capacity. To test residual oxygen consumption, the cells were treated with antimycin-A which inhibits electron flow and is a measure of oxygen consumption due to non-mitochondrial processes. Residual oxygen consumption was less than 0.5% of ETS capacity, signifying that oxygen consumption unrelated to respiration is minimal (Figure 3A). H_2O_2 production increased during OxPHOS compared to when the cells were not being provided with substrates (P=0.004), showing that ROS production increased during OxPHOS (Figure 3E).

PCM: To test FAO, C2C12 myoblasts were provided with a saturating level of F-linked substrate (palmitoyl-carnitine). Malate was provided to support F-linked respiration. Maximal FAO was stimulated with saturating concentrations of ADP (Figure 4A).

Mitochondrial membrane integrity was verified by small changes in respiration after the addition of cytochrome c (<15±9% increase, Figure 4A). Oligomycin was used to inhibit ATP synthase and stimulate a leak state in which oxygen consumption was 9.5±2.8% of maximal OxPHOS (Figure 4B), indicating that during FAO a small component of oxygen consumption can be attributed to dissipation of the proton gradient created by the ETS. Treatment with FCCP was used to test ETS capacity. This resulted in increased oxygen consumption above maximal OxPHOS, demonstrating that ETS capacity exceeds that of OxPHOS during FAO (Figure 4A,B). To test residual oxygen consumption, the cells were treated with antimycin-A. This resulted in a decrease in oxygen consumption to less than 1% of ETS capacity, signifying that oxygen consumption unrelated to respiration is minimal (Figure 4A). H_2O_2 production increased during OxPHOS compared to when the cells were not being provided with F-linked substrate (P=0.03), showing that ROS production is increased during FAO (Figure 4C).

RP2: To test the contribution to respiration from the different pathways to the Q-junction in the ETS, C2C12 myoblasts were provided with saturating F+N+S+Gp-linked substrates sequentially and ADP to stimulate OxPHOS. F-linked respiration (octanoyl-carnitine) contributed 36±2% to maximal OxPHOS capacity (Figure 5C). A low dose of malate was provided to confirm that F-linked respiration was not limited by lack of support through N-linked respiration. Mitochondrial membrane integrity was verified by a lack of increase in respiration after the addition of cytochrome c (<10% increase, P=0.298 for Oct vs. Cyto, Figure 5A). There was a significant increase in respiration after the titration of N-linked substrate (high concentration of malate, Figure 5A). Additional titration of N-linked substrate pyruvate also increased respiration (Figure 5A). The third addition of N-linked substrate glutamate increased respiration, but only by less than 5% (Figure 5A). Neither addition of S-linked substrate (succinate) nor Gp-linked (glycerol phosphate) significantly increased respiration (Figure 5C). FCCP was used to test ETS capacity, resulting in an increase in oxygen consumption that greatly exceeded maximal OxPHOS (Figure 5B). Treatment with rotenone was used to determine the contribution complex I makes to ETS capacity. This decreased ETS capacity by 19±4% (Figure 5D), indicating that S and Gp-linked substrates can make substantial contributions to ETS function, despite the minimal increase in OxPHOS observed when these substrates were added. To test residual oxygen consumption, the cells were treated with antimycin-A. This resulted in a decrease in oxygen consumption to less than 0.5% of ETS capacity, signifying that oxygen consumption unrelated to respiration is minimal (Figure 5A).

Western Blot

Western blot techniques were used to determine the content of complexes in the ETS. The C2C12 cells tested positive for subunits of Complexes I-V of the electron transport system (Figure 6), but comparisons cannot be made due to potential differences in antibody binding affinity for each complex subunit.

Figure 3. Oxygen consumption (JO_2) was measured during GMS (N+S-Linked) mitochondrial respiration, 1 million cells per chamber (2 chambers per run, n=6). **A)** O_2 consumption after the addition of each substrate, uncoupler, or inhibitor. **B)** Components of respiration. **C)** Contribution to OxPHOS from different substrates. **D)** ETS capacity before and after inhibition of complex I with rotenone. **E)** H_2O_2 measurement before and during OxPHOS. P-values are for pair wise comparisons following P<0.05 for main effect of ANOVA. Data are mean and standard deviation

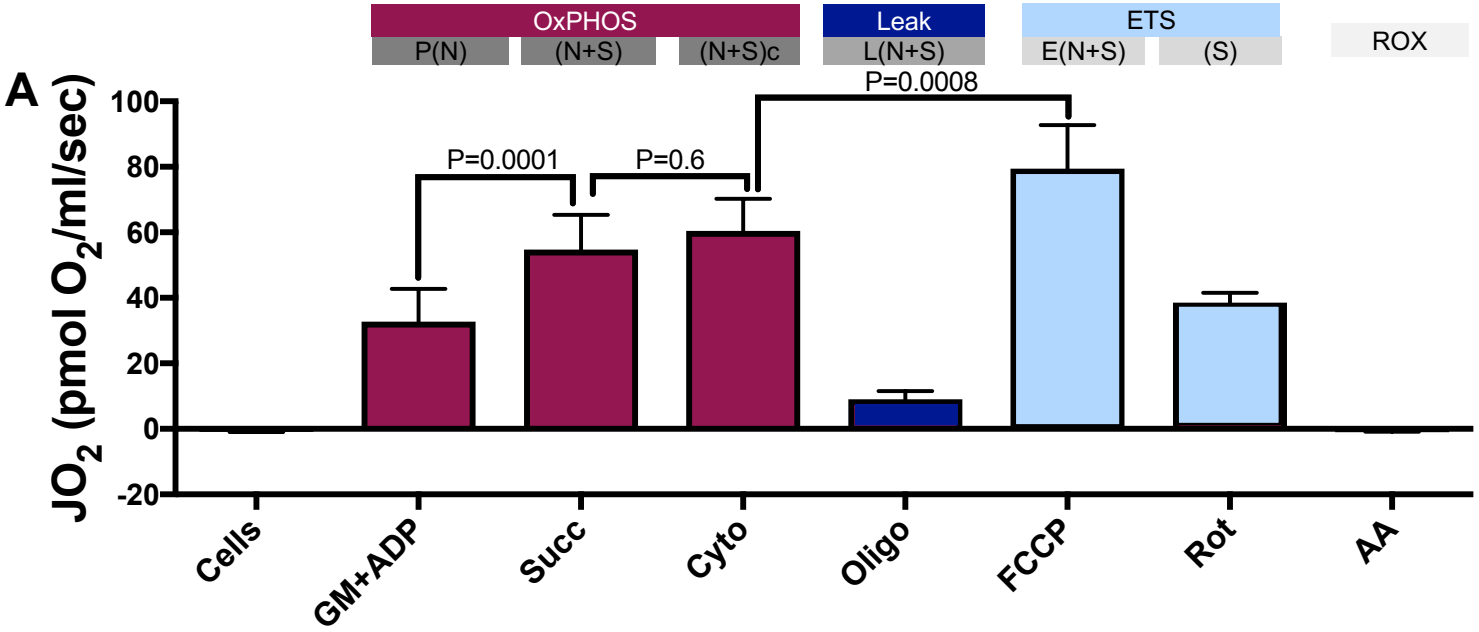

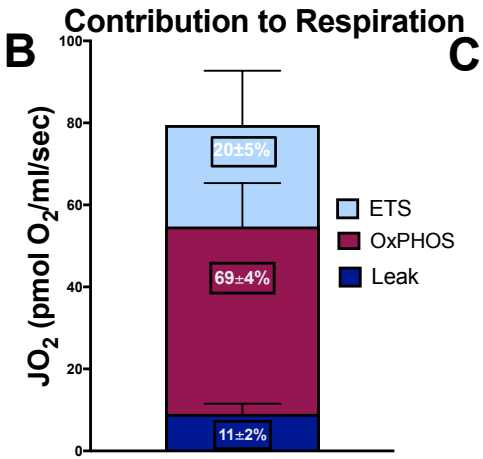

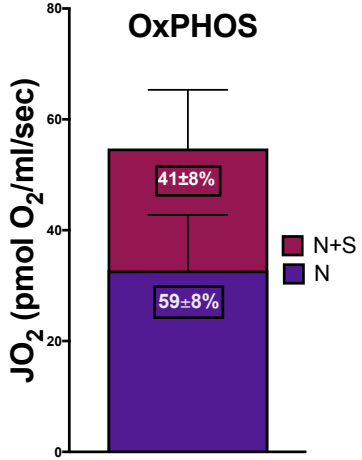

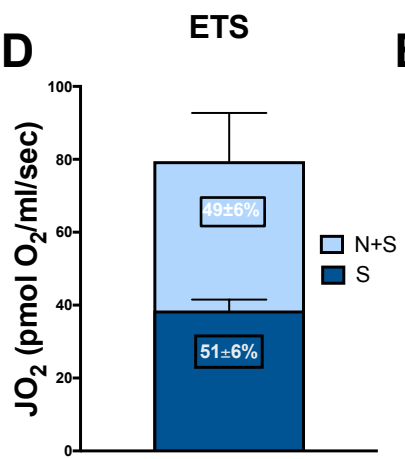

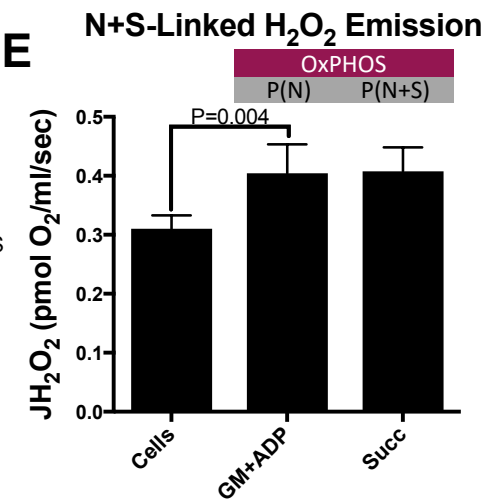

Figure 4. Oxygen consumption (JO_2) was measured during PCM (F-Linked) Fatty acid respiration. 1 million cells per chamber, 2 chambers per run (n=6). **A)** O_2 consumption after the addition of each substrate, uncoupler, or inhibitor. **B)** Components of respiration. **C)** H_2O_2 production measured before and during OxPHOS. P-values are for pair wise comparisons following P<0.05 for main effect of ANOVA. Data are mean and standard deviation.

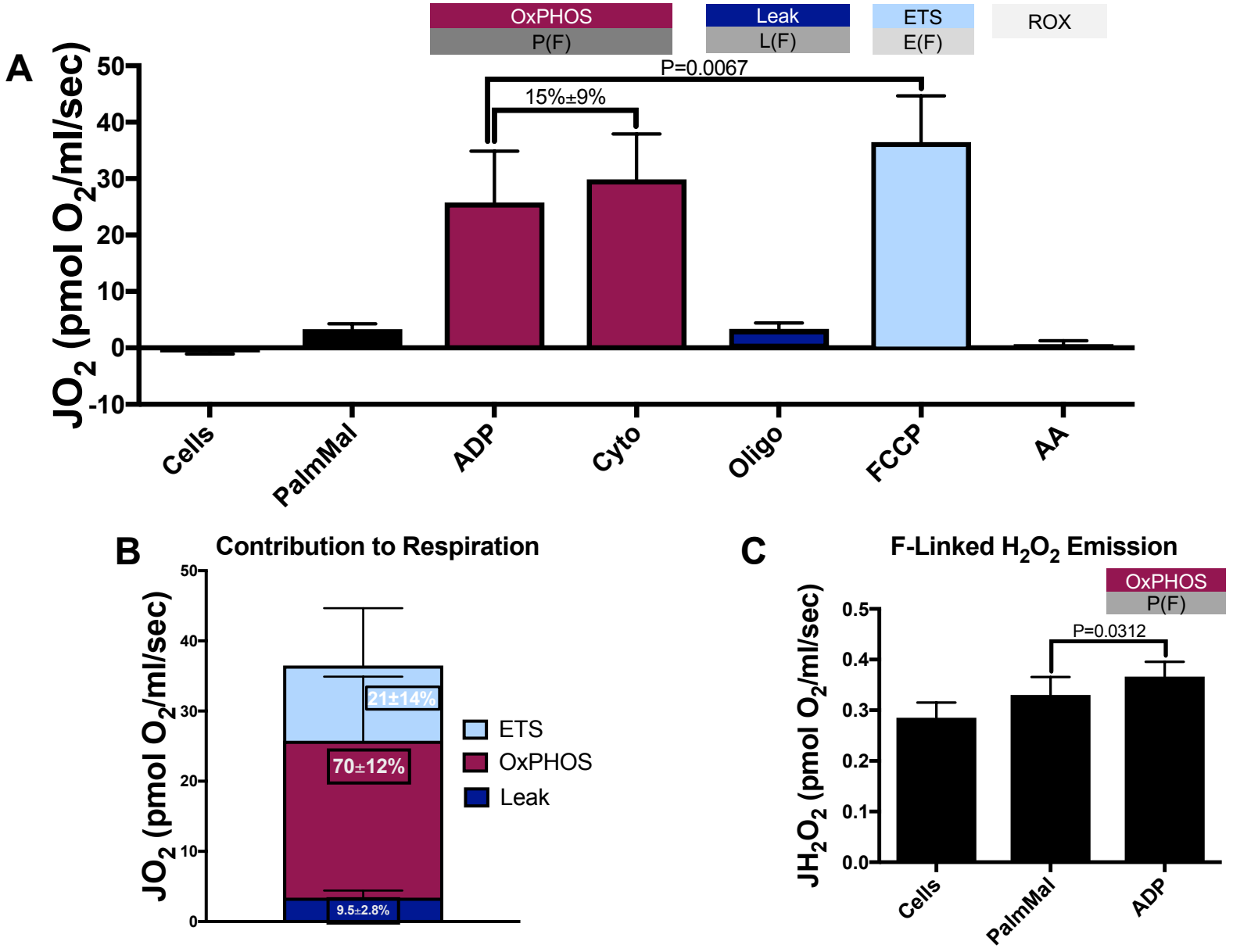

Figure 5. Oxygen consumption (JO_2) was measured during RP2 which measures the contribution to respiration from the different pathways to the Q-junction in the ETS. 1 million cells per chamber, 2 chambers per run (n=6) **A)** O_2 consumption after the addition of each substrate, uncoupler, or inhibitor. **B)** Conmponents of respiration. **C)** Contribution to OxPHOS from each substrate. **D)** ETS capacity before and after inhibition of complex I with rotenone. P-values are for pair wise comparisons following P<0.05 for main effect of ANOVA. Data are mean and standard deviation.

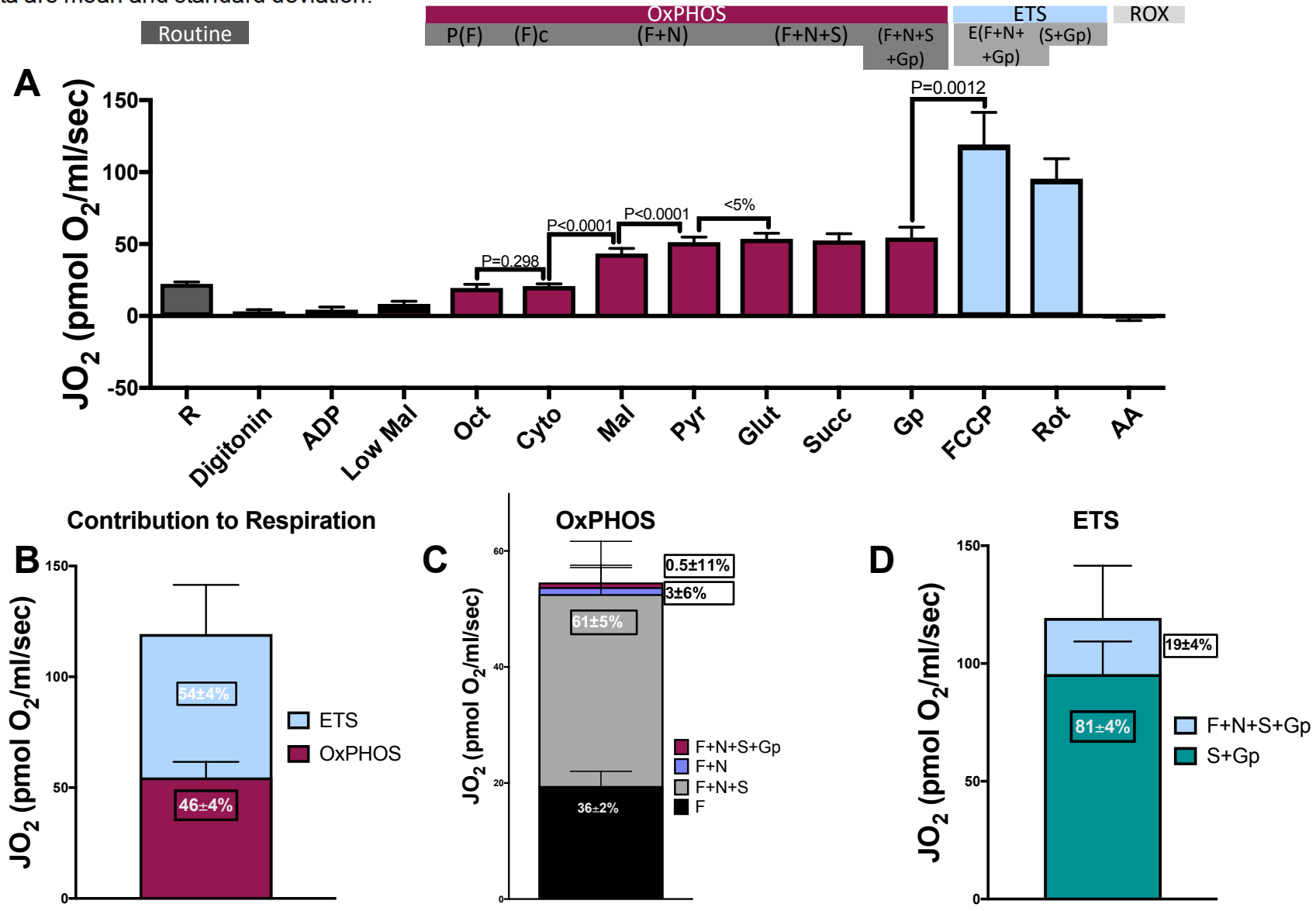

Figure 6. A) Western blot data for C2C12 myoblast detection of OxPHOS cocktail to determine presence of ETS complexes. **B)** Representative blot.

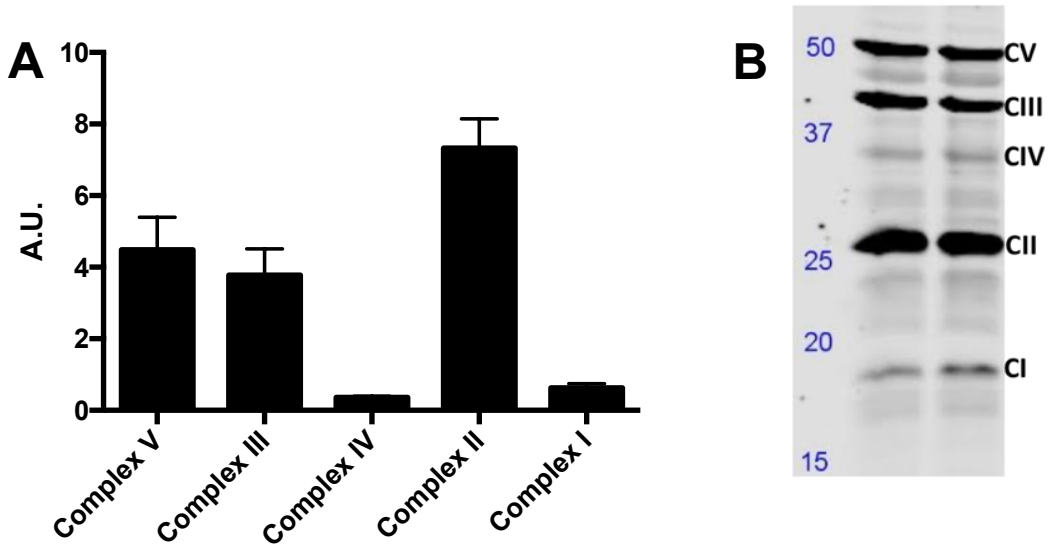

DISCUSSION

The primary purpose of this study was to characterize the cellular respiration and mitochondrial metabolism of C2C12 mouse myoblasts and determine relative contribution of lipid and non-lipid substrates to respiration. This characterization will serve as a reference for the interpretation of further studies using this cell line to study mechanisms of IR. With the use of high-resolution respirometry, we were able to complete respiration profiles of the C2C12 myoblasts. The myoblasts exhibited reduced respiration in the presence of fatty acids in the PCM protocol, demonstrating they have a low intrinsic capacity to oxidize lipids. In the GMS protocol, respiration with N and S-linked substrates exceeded FAO, indicating a relatively greater capacity to oxidize non-lipid substrates can drive respiration in these cells. The reduced FAO was also observed in the RP2 protocol; FAO contributed to 36% of maximal OxPHOS and N-linked substrates contributed 61%. In each protocol performed, OxPHOS capacity was exceeded by ETS capacity, indicating there is a limitation to OxPHOS capacity that is not substrate specific (not only N+S-linked or F+N-linked). This data will enable us to interpret potential changes in respiration patterns in IR states in future studies.

Our observations indicate that multiple protocols are needed to generate a comprehensive respiration profile of the myoblasts. After each substrate addition, the respiration is the net result of all previous additions and any increase in oxygen consumption is the minimal contribution to respiration from that substrate. It is possible the addition of that substrate could be driving respiration entirely. The order of titration is an important consideration. For example, in RP2, after each additional N-linked substrate is titrated, the additive contribution of each substrate can be determined by any change to respiration, but the individual contribution cannot be distinguished. Therefore, when sequential titrations are made it is not possible to determine which substrate is driving respiration. To resolve this issue, it is necessary to run multiple protocols that add substrates in different orders and combinations. For example, in RP2, addition of saturating S-linked substrate (succinate) did not increase respiration. This could suggest that S-linked substrate is does not contribute to respiration. However, the GMS protocol demonstrated that succinate can support respiration in C2C12 cells. Furthermore, inhibition of complex I (where N and F-linked substrates feed into the Q-junction) with rotenone only decreased ETS capacity by 19%, indicating the cells readily oxidize S and Gp-linked substrates. Taken together, these data illustrate that multiple protocols provide a more complete respiration profile.

An understanding of the intrinsic cellular respiration and mitochondrial metabolism of model systems commonly used to study IR and T2D is needed because the dysfunction of respiration has been implicated in the development of IR, but mechanisms remain in question. Mitochondrial dysfunction is a broad term that may refer to a variety of impairments including reduced OxPHOS capacity, increased production of ROS, reduced mitochondrial content, and decreased mitochondrial flexibility as shown by decreased ability for mitochondria to shift metabolism between fuel sources (Montgomery 2015). Mitochondrial size and function have been positively correlated to insulin sensitivity (Kelley 2002). Studies have demonstrated that mitochondrial dysfunction has been observed in IR and T2D, but mechanisms remain in question.

Skeletal muscle is the principal site of insulin-stimulated glucose disposal. Approximately 80% of postprandial glucose disposal occurs in skeletal muscle, thus making it necessary for normal insulin-stimulated whole-body glucose uptake (Gonzalez 2017). Skeletal muscle is also a principal determinant of whole-body glucose metabolism, and displays remarkable capacity for alterations in mitochondrial metabolism (Robinson 2017). It also has a very high content of mitochondria, relying heavily on oxidative phosphorylation for the production of energy (Kelley 2002). When muscle mitochondria can no longer easily switch between oxidizing fat to glucose it impedes their ability to be the major glucose sink, implicating dysfunctional muscle mitochondria in IR. Skeletal muscle IR is one of the first defects seen before T2D. In studies conducted on non-obese normal glucose tolerant offspring of two parents with T2D, there has been observed decreased glucose uptake in response to insulin. This reduction was mostly accounted for by reduced glycogen synthesis; no defect was seen in hepatic glucose production, indicating the defect in insulin action is localized to skeletal muscle (DeFronzo 2009). Compensatory hyperinsulinemia can maintain normal glucose concentration despites declines in insulin action. Over time, the hyperinsulinemia cannot overcome further declines in insulin action and results in hyperglycemia with overt type 2 diabetes (DeFronzo 2010).

There are numerous hypotheses linking skeletal muscle mitochondrial dysfunction to IR. Mitochondria are the primary sites of FAO. Obesity is associated with an increased dependence on FAO that may contribute to excessive lipid accumulation in cells. These lipids can react with the inner mitochondrial membrane and interfere with electron transfer activity, increasing ROS production (Di Meo 2017) and causing mitochondrial damage. The generation of ROS by skeletal muscle mitochondria has been implicated in the development of IR (Anderson 2009).

ROS are by-products of cellular respiration that are produced as a result of high oxygen content and electron flow through the mitochondria, predominantly produced by Complexes I, II and III of the ETS (Di Meo 2017). ROS are necessary for normal mitochondrial function, but an elevation in mitochondrial ROS can cause damage to lipids, DNA, proteins and alter transcriptional regulation (Gonzalez 2017). Uncoupling of the mitochondria can also lead to increased ROS production, and is linked to excess fatty acids. Uncoupling is the inefficient transfer of electrons leading to decreased phosphorylation of ATP per oxygen consumed. Nutrient oversupply increases the inner mitochondrial membrane potential, and without an increase in ATP demand, increased uncoupling occurs. This nutrient oversupply is a hallmark of obesity and T2D (Hesselink 2016).

Increased production of ROS could contribute to IR through their regulation of mitochondrial processes, called dynamics. Mitochondrial dynamics are involved in the upkeep of the mitochondrial network and include the processes of fusion and fission. If these processes are altered, the function and content of the mitochondria may be impaired, resulting in mitochondrial dysfunction. Long-term defects in dynamics have been associated with IR (Hesselink 2016). Altered levels of fission are known to be involved in IR; ROS can be increased in the presence of fission or ROS itself can regulate the level of fission (Di Meo 2017). In C2C12 cells, treatment with palmitate has been observed to increase fission and ROS, resulting in IR. But upon inhibiting fission, insulin sensitivity was improved (Jheng 2011). This demonstrates the need for an

understanding of the intrinsic ROS production in this cell line. We measured ROS production during respiration and did not detect major differences between lipid and non-lipid substrates. Greater ROS production may therefore be a secondary response in insulin resistant models or a net effect from lower endogenous anti-oxidant enzymes (Anderson 2009), and not an intrinsic difference between respiratory substrates.

Alterations in the level FAO leading to lipid accumulation in muscle has been noted as a potential source of mitochondrial dysfunction. Lipid metabolite accumulation could be caused by reduced FAO that results in the accumulation of incomplete products of FAO. These products accumulate when excess nutrient supply increases FAO relative to the demand of energy; these products may also cause oxidative stress and reduced mitochondrial oxidative capacity (Gonzalez 2017).

It is also possible that excess FAO in skeletal muscle leads to the accumulation of lipid metabolites. It has been observed that rodents on a high fat diet accumulate lipid intermediates of FAO and inhibition of FAO prevents this accumulation (Koves 2008). Upon inhibiting FAO, treatment of myocytes with fatty acids could not inhibit insulin sensitivity compared to control fatty acid condition (Koves 2008), implicating excess FAO in the development of IR.

It has also been observed that overall fat oxidation rates can show no changes, but high rates of incomplete fat oxidation can occur in rodents on a high fat diet (Koves 2008), leading to incomplete FAO products as the potential culprit. We identified that C2C12 myoblasts exhibit a low intrinsic capacity to oxidize lipids relative to total ETS capacity or OxPHOS of N and S-linked substrates. Any potential limitation of FAO may be due to lipid-specific pathways (such as beta-oxidation) and less so for more general pathways (such as the ETS). Knowing this will be important in future studies that aim to determine potential limitations or excess states of FAO during IR.

Other impairments that have been hypothesized to link mitochondrial dysfunction and IR include a low intrinsic respiration and reduced mitochondrial flexibility. A low intrinsic respiration could predispose some individuals to be more susceptible to IR. There has been evidence to suggest inner mitochondrial membrane proteins could be responsible for variation in metabolic rate among humans (Hesselink 2016). Mitochondrial flexibility is necessary for healthy mitochondria to switch between oxidizing different substrates such as glucose in postprandial state with high insulin versus fatty acids in postabsorptive state with low insulin (Hesselink 2016). Mitochondria harvested from high fat fed rats exhibit inability to switch to glucose derived substrates upon exposure to pyruvate, whereas rats fed on “standard chow” were able to inhibit FAO. The high fat fed mice could not inhibit FAO, indicating that muscle mitochondria exhibit an inability to switch substrates on a high fat diet (Koves 2008). In the current study, we demonstrated the C2C12 myoblasts exhibited an ability to switch fuel sources, indicating the mitochondria have a capacity to switch between metabolic fuels.

It is important to consider the assumptions and limitations of the O2k. Oxygen consumption is primarily due to mitochondrial respiration, but other pathways can contribute to total cellular oxygen consumption. We quantified non-mitochondrial respiration following inhibition of the respiratory chain with antimycin-A and determined very little contribution to overall oxygen consumption. Another consideration is that the conditions within the O2k are not physiologic, as substrates are provided in saturating

concentrations and respiration is determined under maximal conditions, which may exceed *in vivo* energy requirements. Furthermore, the cells have been disrupted and removed from their growth environment. Membrane integrity was confirmed by determining the change in respiration after titration of cytochrome c. However, the cellular membrane was permeabilized with digitonin to provide free diffusion of substrates into the cells, and intracellular components will diffuse out of the cell (e.g. glycolytic enzymes). Lastly, respiration was measured in myoblasts, which are undifferentiated muscle cells. There is potential that respiration could be higher or lower in differentiated cells, but due to a loss of membrane integrity in differentiated muscle cells it is not possible to measure their respiration in the O2k. An alternative to the O2k for measuring mitochondrial metabolism is the Seahorse XF extracellular flux analyzer. The Seahorse XF can measure respiration when the cells are still attached to the plate (Horan 2012), allowing for measurements on undisrupted cells. However, only four substrates can be injected when using the Seahorse XF. This does not allow for a full characterization of the cell line (Horan 2012). The O2k permits longer titration sequences for comprehensive respiratory analysis.

In conclusion, it is necessary to characterize cellular respiration and mitochondrial metabolism in C2C12 myoblasts because they are commonly used to study IR and T2D, and mitochondrial dysfunction has been implicated in these disease states. Understanding the relative capacity of oxidative phosphorylation to electron transfer system also provides insight into potential limitations of cellular respiration. Our data indicate that C2C12 myoblasts respire normally using both lipid and non-lipid substrates. We observed no mitochondrial defects using different substrates and titration sequences, indicating these cells are effective models to study cellular respiration. We also observed that when using high-resolution respirometry it is necessary to perform multiple protocols in order to create a complete respiration profile of the cells in question. Future considerations are to compare the C2C12 myoblast respiration patterns to other cell models and human cells. Furthermore, treatment with fatty acids can model IR to further understand the alterations that may occur with mitochondrial respiration.

ACKNOWLEDGEMENTS

I would like to thank doctoral students in the Translational Metabolism Research Laboratory Harrison Steirwalt and Sarah Ehrlicher for their support in running respiratory experiments, culturing cells, and running statistical software. I would also like to thank Emily Burney for her contributions to the project and the College of Science for the SURE scholarship I received to work on this project over the summer. Last but not least, I would like to thank my mentors committee members Sean Newsom, Matt Robinson, and Indira Rajagopal for their teaching and support throughout the project.

REFERENCES

Anderson, E., Lustig, M., Boyle, K., Woodlief, T., Kane, D., Lin, C., Price, J., Kang, L., Rabinovitch, P., Szeto, H., Houmard, J., Cortright, R., Wasserman, D., Neufer, D. (2009). Mitochondrial H_2O_2 emission and cellular redox state link excess fat intake to insulin

resistance in both rodents and humans. *Journal of Clinical Investigation,* vol. 119, pp. 573-581. Retrieved from: https://www.jci.org/articles/view/37048

Befroy, D., Peterson, K., Dufour, S., Mason, G., de Graaf, R., Rothman, D., Shulman, G. (2007). Impaired mitochondrial substrate oxidation in muscle of insulin-resistant offspring of type 2 diabetic patients. *Diabetes,* vol. 56(5), pp. 1376-1381. Retrieved from: http://diabetes.diabetesjournals.org/content/56/5/1376.long

Covington, J., Johannsen, D., Coen, P., Burk, D., Obanda, D., Ebenezer, P., Tam, C., Goodpaster, B., Ravussin, E., Bajpeyi, S. (2017). Intramyocellular Lipid Droplet Size Rather Than Total Lipid Content is Related to Insulin Sensitivity After 8 Weeks of Overfeeding. *Obesity,* vol. 25(12), pp. 2079-2087. Retrieved from: https://onlinelibrary.wiley.com/doi/abs/10.1002/oby.21980

DeFronzo, R., Abdul-Ghani, M. (2010). Pathogenesis of Insulin Resistance in Skeletal Muscle. *Journal of Biomedicine and Biotechnology.* Retrieved from: https://www.ncbi.nlm.nih.gov/pmc/articles/PMC2860140/

DeFronzo, R., Tripathy, D. (2009). Skeletal Muscle Insulin Resistance Is the Primary Defect in Type 2 Diabetes. *Diabetes Care,* vol. 32(2), pp. 157-163. Retrieved from: https://www.ncbi.nlm.nih.gov/pmc/articles/PMC2811436/pdf/zdcS157.pdf

Di Meo, S., Iossa, S., Venditti, P. (2017). Skeletal muscle insulin resistance: role of mitochondria and other ROS sources. *Journal of Endocrinology,* vol. 233(1), pp. 15-42. Retrieved from: http://joe.endocrinology-journals.org/content/233/1/R15.figures-only?related-urls=yes&legid=joe;233/1/R15

Gnaiger, E. (2014). *Mitochondrial Pathways and Respiratory Control.* Innsbruck, Austria: Oroboros Instruments Corp MiPNet Publications.

Gonzalez-Franquesa, A., Patti, M. (2017). Insulin Resistance and Mitochondrial Dysfunction. In: Santulli G. (eds) Mitochondrial Dynamics in Cardiovascular Medicine. Advances in Experimental Medicine and Biology, vol 982, (pp. 465-520). Springer, Cham.

Hancock, C., Han, D., Chen, M., Terada, S., Yasuda, T., Wright, D., Holloszy, J. (2008). High-fat diets cause insulin resistance despite an increase in muscle mitochondria. *Proceedings of the National Academy of Sciences of the United States of America,* vol. 105(22), pp. 7815-7820. Retrieved from: http://www.pnas.org/content/105/22/7815.long

Hesselink, M., Schrauwen-Hinderling, V., Schrauwen, P. (2016). Skeletal muscle mitochondria as a target to prevent or treat type 2 diabetes mellitus. *Nature Review*s, vol. 67(10), pp. 1022-1035. Retrieved from: https://www.nature.com/articles/nrendo.2016.104

Horan, M., Pichaud, N., Ballard, W. (2012). Review: Quantifying Mitochondrial Dysfunction in Complex Diseases of Aging. *Journal of Gerontology,* vol. 67(10), pp. 1022-1035. Retrieved from: https://academic.oup.com/biomedgerontology/article/67/10/1022/530752

Jheng, H., Tsai, P., Guo, S., Kuo, L., Chang, C., Su, I., Chang, CR., Tsai, Y. (2011). Mitochondrial Fission Contributes to Mitochondrial Dysfunction and Insulin Resistance in Skeletal Muscle. *Molecular and Cellular Biology,* vol. 32(2), pp. 309-319. Retrieved from: https://www.ncbi.nlm.nih.gov/pmc/articles/PMC3255771/

Kelley, D., He, J., Menshikova, E., Ritov, V. (2002). Dysfunction of Mitochondria in Human Skeletal Muscle in Type 2 Diabetes. *Diabetes,* vol. 51(10), pp. 2944-2950. Retrieved from: http://diabetes.diabetesjournals.org/content/51/10/2944

Koves, T., Ussher, J., Noland, R., Slentz, D., Mosedale, M., Ilkayeva, O., Bain, J., Stevens, R., Dyck, J., Newgard, C., Lopaschuk, G., Muoio, D. (2008). Mitochondrial Overload and Incomplete Fatty Acid Oxidation Contribute to Skeletal Muscle Insulin Resistance. *Cell Metabolism,* vol. 7, pp. 45-56. Retrieved from: http://www.cell.com/cell-metabolism/fulltext/S15504131(07)003063?_returnURL=https%3A%2F%2Flinkinghub.elsevier.com%2Fretrieve%2Fpii%2FS1550413107003063%3Fshowall%3Dtrue

Lalia, A., Dasari, S., Johnson, M., Robinson, M., Konopka, A., Distelmaier, K., Port, J., Glavin, M., Esponda, R., Nair, K., Lanza, I. (2016). Predictors of Whole-Body Insulin Sensitivity Across Ages and Adiposity in Adult Humans. *The Journal of Clinical Endocrinology & Metabolism,* vol. 101(2), pp. 626-634. Retrieved from: https://academic.oup.com/jcem/article/101/2/626/2810955

Lanza, I., Blachnio-Zabielska, A., Johnson, M., Schimke, J., Jakaitis, D., Lebrasseur, N., Jensen, M., Sreekumaran Nair, K., Zabielski, P. (2013). Influence of fish oil on skeletal muscle mitochondrial energetics and lipid metabolites during high-fat diet. *American Journal of Physiology-Endocrinology and Metabolism,* vol. 304(12), pp. E1391-E1403. Retrieved from: https://www.ncbi.nlm.nih.gov/pmc/articles/PMC4116354/

Montgomery, M., Turner, N. (2015). Mitochondrial dysfunction and insulin resistance: an update. *Endocrine Connections,* vol. 4(1), pp. 1-15. Retrieved from: http://www.endocrineconnections.com/content/4/1/R1.abstract

Newsom, S., Miller, B., Hamilton, K., Ehrlicher, S., Stierwalt, H., Robinson, M. (2017). Long-term rates of mitochondrial protein synthesis are increased in mouse skeletal muscle with high fat feeding regardless of insulin sensitizing treatment. *American Journal of Physiology,* vol. 313(5), pp. E552-E562.

Oroboros. (2018, April 18). 1D;2M;3Oct;4M;5P;6G;7S;8Gp;9U;10Rot-. Retrieved from: http://wiki.oroboros.at/index.php/1D;2M;3Oct;4M;5P;6G;7S;8Gp;9U;10Rot-

Rizza, R., Mandarino, L., Gerich, J. (1981). Dose-response characteristics for effects of insulin on production and utilization of glucose in man. *American Journal of Physiology,* vol. 240(6), pp. E630-E639. Retrieved from: https://www.physiology.org/doi/abs/10.1152/ajpendo.1981.240.6.E630?url_ver=Z39.88-2003&rfr_id=ori%3Arid%3Acrossref.org&rfr_dat=cr_pub%3Dpubmed

Robinson, M., Dasari, S., Konopka, A., Johnson, M., Manjunatha, S., Esponda, R., Carter, R., Lanza, I., Nair, K. (2017). Enhanced Protein Translation Underlies Improved Metabolic and Physical Adaptations to Different Exercise Training Modes in Young and Old Humans. *Cell Metabolism,* vol. 25(3), pp. 581-592. Retrieved from: https://www.cell.com/cell-metabolism/fulltext/S1550-4131(17)30099-2